



Geophysical Research Letters

Supporting Information for

Discrepant estimates of primary and export production from satellite algorithms, a biogeochemical model, and geochemical tracer measurements the North Pacific Ocean

Hilary I. Palevsky^{1a}, Paul D. Quay¹, David P. Nicholson²

¹School of Oceanography, University of Washington, Seattle, Washington, USA

²Marine Chemistry and Geochemistry Department, Woods Hole Oceanographic Institution, Woods Hole, Massachusetts, USA

^aCorresponding Author:

School of Oceanography, University of Washington, Seattle, Washington 98105, USA

Email: palevsky@uw.edu

Contents of this file

Text S1 – Uncertainty estimates

Table S1 – Data sources

Table S2 – Spatial and interannual variability of satellite data at time series stations

Figure S1 – E-ratio and EP trends with depth

References

Text S1: Uncertainty estimates

An overview of the data sources and methodological approaches for the geochemical-, satellite-, and model-based estimates included in the paper is provided in Table S1. To evaluate agreement among these methods, uncertainty bounds are calculated for the geochemical estimates and the satellite- and model-based estimates are considered to agree with the geochemical estimates if they fall within those uncertainty bounds. For the satellite- and model-based estimates, we do not attempt to estimate methodological uncertainty, which is not well defined.

In the container ship regions, uncertainty in the geochemical estimates represents methodological uncertainty from both error in the geochemical tracer (triple oxygen isotope and O₂/Ar dissolved gas ratio) measurements and from uncertainty introduced from each additional term included in the mass balance budgets to calculate gross oxygen and net community production (GOP and NCP, with mass balance budgets including terms for the rate of air-sea gas transfer and physical transport of the measured tracers). For full details of the uncertainty calculations and mass balance budgets, see *Palevsky et al.* [2016]. Methodological uncertainty in seasonal and annual NCP and GOP rates (shown in Figures 3 and 4) ranges from 13% to 36% in the container ship regions.

At the time-series stations, geochemical estimates are available from many previous studies and uncertainty is presented as the standard deviation of all previous geochemical-based estimates, allowing us to compile results from many studies using a variety of methodological and data interpolation approaches. This follows the approach previously taken by *Emerson* [2014] in compiling results for annual NCP (4 studies at OSP and 8 studies at ALOHA) and by *Palevsky et al.* [2016] in compiling results for annual PP at OSP (3 studies). Annual PP at ALOHA was compiled directly from Hawaii Ocean Times-Series data for this study (details in Table S1), and we represent uncertainty as the standard deviation over estimates from all years 2003-2013. The uncertainties derived from this approach (24-28% for annual NCP and 20%-22% for annual PP) are greater than the methodological uncertainties for annual NCP and PP estimates in the Eastern container ship region, most directly comparable to OSP and ALOHA.

A potential additional consideration in comparing the geochemical estimates with satellite and model data is the influence of spatial and temporal variability in appropriately aligning estimates from each method. For the comparison presented in this paper focusing on climatological mean values on seasonal and annual time scales, this issue is largely mitigated by the large number of data points compiled within each seasonal or annual estimate. Results are not sensitive to the choice of spatial box size used to extract the satellite and model data around each geochemical sampling point, demonstrated based on analysis of satellite data (available at 1/6° resolution) at Ocean Station Papa and Station ALOHA over a range of spatial box sizes from 1/6° to 4°, which have minimal effect on climatological mean annual results and a significantly smaller effect than interannual variability (Table S2).

Table S1: Data sources.

| | Primary production (PP) | e-ratio (EP/PP) | Export production (EP) |
|---|--|---|--|
| <i>Geochemistry: Time-series sites</i> | ¹⁴ C-PP incubations ^a | Determined from EP and PP | Oxygen, carbon and nitrate annual mass balance (<i>Emerson</i> [2014], Table 2) |
| <i>Geochemistry: Container ship regions</i> | Triple oxygen isotope budgets ^b | Determined from EP and PP | O ₂ /Ar dissolved gas ratio budgets ^b |
| <i>Satellite-based algorithms</i> | VGPM [<i>Behrenfeld and Falkowski</i> , 1997] and CbPM [<i>Westberry et al.</i> , 2008] ^c | <i>Laws et al.</i> [2000]; <i>Dunne et al.</i> [2005, 2007]; and <i>Henson et al.</i> [2011] ^c | Determined from all combinations of satellite-based PP and e-ratio algorithms |
| <i>Global biogeochemical model</i> | CESM1-BEC climatological year ^d | CESM1-BEC climatological year ^d | CESM1-BEC climatological year ^d |

^a Ocean Station Papa data are from 24-hour incubations (compiled in *Palevsky et al.* [2016], Table 3). Station ALOHA data are from 12-hour dawn to dusk incubations on monthly Hawaii Ocean Time-series (HOT) cruises from 2003-2013 (available from <http://hahana.soest.hawaii.edu/hot/hot-dogs>) integrated to 125 meters following the trapezoid method and scaled to a 24-hour incubation equivalent NPP rate assuming a 15% respiration rate from dusk to dawn [*Karl et al.*, 1996].

^b Gross oxygen production (GOP) to the base of the seasonal mixed layer and the euphotic zone and EP to the base of the seasonal mixed layer, compensation depth, and winter ventilation depth calculated based on mixed layer geochemical measurements on 16 container ship cruises [*Palevsky et al.*, 2016]. GOP is converted to PP using a GOP:NPP ratio of 2.7 and EP is converted from oxygen to carbon units using an O₂:C ratio of 1.4, as in *Palevsky et al.* [2016]. Uncertainty in these estimates represents methodological uncertainty, but not sampling bias within the regions, since satellite and CESM data are sampled at the same times and locations as geochemical measurements (see *Palevsky et al.*, [2016] for details). Seasonal EP is not presented for the winter due to high uncertainty.

^c Moderate Resolution Imaging Spectroradiometer (MODIS) Aqua R2014 monthly satellite products at 1/6° resolution (available from <http://www.science.oregonstate.edu/ocean.productivity>) were downloaded directly for the VGPM and CbPM and used in combination with SST and chlorophyll to calculate e-ratios following the Laws00, Dunne07 and Henson11 algorithms. For a small fraction of years in the MODIS record (2-3), satellite data were unavailable for December at OSP for some variables. Annual records for those years were created using climatological mean December data for all years with available data. A larger spatial box around the time series stations (2.5°) than in the container ship regions (1/3°) was used to reduce the number of years without available December data.

^d Global output from the Parallel Ocean Program of the Community Earth System Model version 1.1.1 (CESM), with the Biogeochemical Ecosystem Component (BEC), run with repeated climatological normal year forcing. Full details of the model configuration are described in *Nicholson et al.* [2014]. Model rates of photosynthesis and respiration in each depth level in each grid cell were used to determine PP both in the mixed layer and throughout the full euphotic zone and EP to the base of the seasonal mixed layer, the community compensation depth, and the winter mixed layer.

Table S2: Spatial and temporal variability of satellite data at time series stations.

| | VGPM (mol C m ⁻² yr ⁻¹) | CbPM (mol C m ⁻² yr ⁻¹) | SST (°C) | Chlorophyll (µg/L) |
|--|--|--|--------------------|------------------------------|
| <i>Ocean Station Papa (OSP)</i> | | | | |
| <i>Climatological annual mean, 2.5 degree box, 2003-2013</i> | 12.9 | 9.2 | 8.1 | 0.33 |
| <i>1σ (Range) over all years^a</i> | 1.3 (10.6-14.9) | 1.3 (8.1-11.4) | 0.6 (7.5-9.3) | 0.04 (0.28-0.42) |
| <i>1σ (Range) over all box sizes^b</i> | 0.4 (12.8-13.7) ^c | 0.1 (9.0-9.2) | 0.01 (8.09-8.12) | 0.004 (0.32-0.33) |
| <i>Station ALOHA</i> | | | | |
| <i>Climatological annual mean, 2.5 degree box, 2003-2013</i> | 8.0 | 14.5 | 25.0 | 0.079 |
| <i>1σ (Range) over all years^a</i> | 0.2 (7.7-8.3) | 1.6 (12.2-16.5) | 0.3 (24.4-25.5) | 0.005 (0.069-0.085) |
| <i>1σ (Range) over all box sizes^b</i> | 0.02 (7.9-8.0) | 0.05 (14.3-14.5) | 0.06 (24.9-25.1) | 0.001 (0.078-0.080) |

^a Interannual variability (over all eleven years from 2003-2013) of climatological annual mean results for a 2.5° box around each station.

^b Climatological annual mean results were calculated using a range of box size choices from 1/6° to 4° (1/6°, 1/3°, 0.5°, 1°, 1.5°, 2°, 2.5°, 3°, and 4°).

^c Higher values (>13.0) do not include any December data (sparse due to winter solar angle and cloud cover and therefore absent in smaller box sizes) and are thus biased high.

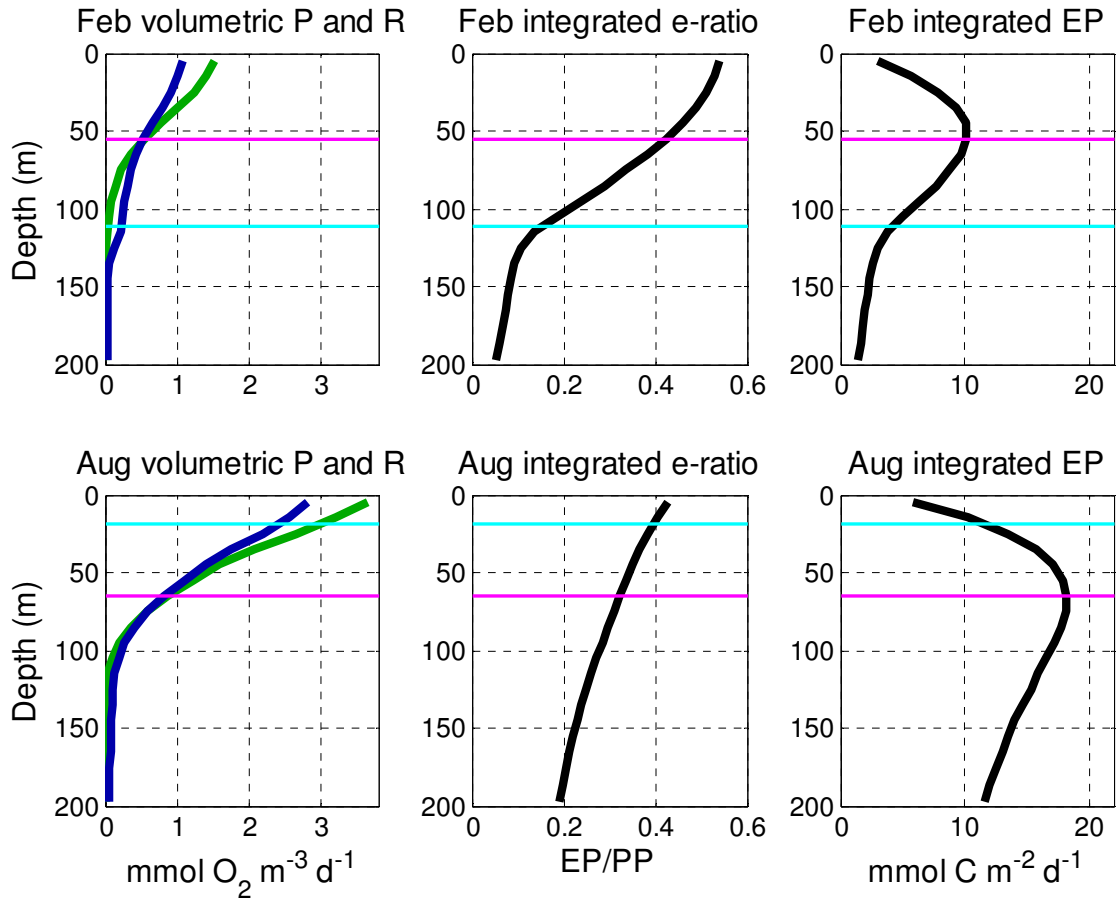


Figure S1. Volumetric photosynthesis (P, green) and respiration (R, blue) rates through the top 200 m of the water column in CESM output (left) are used to calculate export efficiency (e-ratio, EP/PP, center), and export production (EP, right, assumed equal to net community production, or P – R) rates integrated through the water column from the surface down to a range of possible depth criteria up to 200 m. Profiles are shown for both February (top) and August (bottom) for a representative location in the subarctic North Pacific (40°N, 175°E). The community compensation depth (where P and R rates are equal) is shown in magenta and the seasonal mixed layer depth is shown in cyan. Volumetric P and R rates both decrease with depth, but P drops off more steeply than R, such that the depth-integrated e-ratio is greatest at the surface and decreases with deepening depth criteria. The maximum EP from all possible depth criteria is at the compensation depth, since all shallower depths are net autotrophic and all deeper depths are net heterotrophic.

References

- Behrenfeld, M. J., and P. G. Falkowski (1997), Photosynthetic rates derived from satellite-based chlorophyll concentration, *Limnol. Oceanogr.*, *42*(1), 1–20.
- Dunne, J. P., R. A. Armstrong, A. Gnanadesikan, and J. L. Sarmiento (2005), Empirical and mechanistic models for the particle export ratio, *Glob. Biogeochem. Cycles*, *19*, doi:10.1029/2004GB002390.
- Dunne, J. P., J. L. Sarmiento, and A. Gnanadesikan (2007), A synthesis of global particle export from the surface ocean and cycling through the ocean interior and on the seafloor, *Glob. Biogeochem. Cycles*, *21*(4), doi:10.1029/2006GB002907.
- Emerson, S. (2014), Annual Net Community Production and the Biological Carbon Flux in the Ocean, *Global Biogeochem. Cycles*, *28*, doi:10.1002/2013GB004680.
- Henson, S. A., R. Sanders, E. Madsen, P. J. Morris, F. Le Moigne, and G. D. Quartly (2011), A reduced estimate of the strength of the ocean's biological carbon pump, *Geophys. Res. Lett.*, *38*(4), 10–14, doi:10.1029/2011GL046735.
- Karl, D. M., J. R. Christian, J. E. Dore, D. V. Hebel, R. M. Letelier, L. M. Tupas, and C. D. Winn (1996), Seasonal and interannual variability in primary production and particle flux at Station ALOHA, *Deep Sea Res., Part II*, *43*(2-3), 539–568, doi:10.1016/0967-0645(96)00002-1.
- Laws, E., P. Falkowski, W. J. Smith, H. Ducklow, and J. McCarthy (2000), Temperature effects on export production in the open ocean, *Glob. Biogeochem. Cycles*, *14*(4), 1231–1246.
- Nicholson, D., R. H. R. Stanley, and S. C. Doney (2014), The triple oxygen isotope tracer of primary productivity in a dynamic ocean model, *Global Biogeochem. Cycles*, *28*, 538–552, doi:10.1002/2013GB004704.
- Palevsky, H. I., P. D. Quay, D. E. Lockwood, and D. P. Nicholson (2016), The annual cycle of gross primary production, net community production, and export efficiency across the North Pacific Ocean, *Glob. Biogeochem. Cycles*, *30*, doi:10.1002/2015GB005318.
- Westberry, T., M. J. Behrenfeld, D. A. Siegel, and E. Boss (2008), Carbon-based primary productivity modeling with vertically resolved photoacclimation, *Glob. Biogeochem. Cycles*, *22*(2), 1–18, doi:10.1029/2007GB003078.